

# Anomalous phase separation and hidden coarsening of super-clusters in the Falicov-Kimball model

Sheng Zhang, Puhua Zhang, and Gia-Wei Chern

*Department of Physics, University of Virginia, Charlottesville, VA 22904, USA*

(Dated: May 28, 2021)

We show that the celebrated Falicov-Kimball model exhibits rich and intriguing phase-ordering dynamics. Applying modern machine learning methods to enable large-scale quantum kinetic Monte Carlo simulations, we uncover an unusual phase-separation scenario in which the growth of charge checkerboard clusters competes with domain coarsening related to a hidden symmetry-breaking. A self-trapping mechanism as a result of this competition gives rise to arrested growth of checkerboard patterns and their super-clusters. Glassy behaviors similar to the one reported in this work could be generic for other correlated electron systems.

Complex mesoscopic textures are ubiquitous in strongly correlated electron materials [1–8]. Notable examples include stripe and checkerboard patterns in high- $T_c$  superconductors, and nano-scale phase separation in manganites and canonical Mott insulators such as vanadium oxides. Not only are these mesoscopic textures of fundamental importance in correlated electron physics, they are also central to the emergence of novel functionalities in these materials. These nanoscale patterns often come from phase-separation instability driven by electron correlation effects. Indeed, a generic feature of lightly doped Mott insulators is the strong tendency toward phase separation in which the doped holes are expelled from locally insulating antiferromagnetic domains [9–15]. Although considerable efforts have been devoted to understanding mechanisms of phase separation in strongly correlated materials, nonequilibrium pattern-formation dynamics in such systems is poorly understood.

On the other hand, intermediate states with complex structures have been observed in discontinuous phase transitions of many classical systems [16, 17]. The kinetics of first-order transition is a mature subject with a long history [18–20]. In such studies, one concerns the evolution of a system from an unstable or meta-stable state to its preferred equilibrium phase, a process that is often characterized by the emergence of complex spatial-temporal patterns. Several numerical techniques have been developed for large-scale simulations of phase-separation dynamics [21–24]. One key issue is the dynamical universality class and universal growth law [25, 26]. However, most of the works in this field are based on empirical energy models which cannot capture the subtle electron correlation effects. A comprehensive modeling of correlation-driven phase separation thus needs take into account both microscopic electronic processes and mesoscopic pattern formation dynamics.

In this paper we apply modern machine learning methods to enable large-scale simulation of phase separation phenomena in the Falicov-Kimball (FK) model [27], which is one of the canonical correlated electron systems. It describes conducting  $c$ -electrons interact with localized  $f$ -electrons through an on-site repulsive interaction.

Originally put forward as a limiting case of the Hubbard model [28], the FK model was later independently proposed to describe semiconductor-metal transitions in rare-earth and transition-metal compounds [27]. Its relative simplicity allows for numerically exact solutions, which serve as important benchmarks for sophisticated many-body methods [29]. The FK model itself has rich phase diagrams, and is one of the best-studied correlated electron systems that exhibit complex pattern formation and phase separation [30–38].

We consider the spinless FK Hamiltonian on a square lattice [34] in this work

$$\mathcal{H} = -t_1 \sum_{\langle ij \rangle} c_i^\dagger c_j + U \sum_i c_i^\dagger c_i w_i. \quad (1)$$

Here  $c_i^\dagger$  ( $c_i$ ) is the creation (annihilation) operator for a  $c$ -electron at site  $i$ ,  $\langle ij \rangle$  denotes nearest-neighbor pairs on the lattice,  $w_i$  is the occupation number of the  $f$ -electron,  $t_1$  is the nearest-neighbor hopping constant, which also serves as the energy unit, and  $U > 0$  is the strength of on-site repulsive interaction. For convenience, we will also use the terminology of viewing  $w_i = 0$  or 1 as a classical variable that indicates the absence or presence of an “ion” at site- $i$  [34, 35]. Thanks to the quadratic nature of  $c$ -electron Hamiltonian, equilibrium phases of the FK model can in principle be exactly solved numerically by combining classical Monte Carlo method for ions with exactly diagonalization (ED) for  $c$ -electrons [36–38]. Moreover, within the framework of dynamical mean-field theory, the quantum impurity problem associated with the FK model can also be exactly solved [29, 35].

The equilibrium phases of the square-lattice FK model have been extensively studied over the years. Exactly at half-filling for both electrons and ions, the ground-state exhibits a charge density wave (CDW) order with the ions forming a checkerboard pattern [37, 38]. Away from half-filling, the model shows various stripe and incommensurate phases [33, 34]. With slight electron or hole doping, a phase-separated regime is stabilized [34–36], a scenario similar to that in the Hubbard model. Despite being one of the prominent models for electronic phase

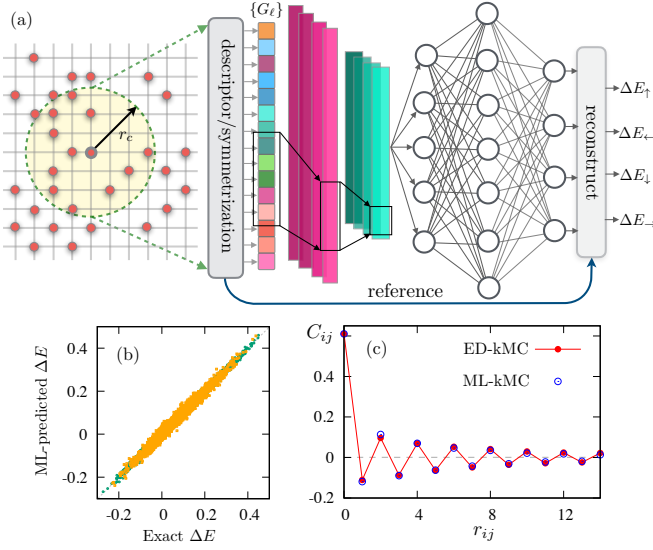


FIG. 1. (a) Schematic diagram of neural-network (NN) energy model for kMC dynamics simulation of the FK system. A descriptor is used to construct effective coordinates  $\{G_\ell\}$  from neighborhood ion configuration  $\{w_j\}$  up to a cut-off  $r_c = 10$ . These feature variables  $\{G_\ell\}$  are input to the NN which predicts the energy differences  $\Delta E$  at the output. (b) ML-predicted  $\Delta E$  versus exact values; the circles and squares denote training and test datasets, respectively. (c) Comparison of ion correlation function obtained from ED and ML-kMC simulations on a  $30 \times 30$  lattice after 5000 steps from the same initial condition.

separation, the phase-ordering dynamics in FK system has never been studied. As a result, important questions, such as whether the system exhibits dynamical scaling and what is the domain-growth law, remain open.

To address these issues, we formulate a kinetic Monte Carlo (kMC) method [23, 39] to simulate phase ordering of the FK model subject to a temperature quench. While the  $c$ -electrons have well-defined dynamics in the FK Hamiltonian, the ions  $w_i$  are static variables, similar to classical Ising spins. To endow the ions with a dynamics, a random-walk algorithm is used to model their diffusive motion. At every time-step, attempt is made to move a randomly chosen ion to one of its empty neighbors. Whether the update is accepted is determined by the standard Metropolis criterion [23]. We further assume that the equilibration of  $c$ -electrons is much faster compared with the random walks of ions, analogous to Born-Oppenheimer approximation in quantum molecular dynamics [40]. The acceptance probability of such a nearest-neighbor move is  $p_{i \rightarrow j} = \frac{1}{4} \min(1, e^{-\Delta E_{i \rightarrow j}/k_B T})$ , where  $\Delta E_{i \rightarrow j}$  is the free-energy difference of  $c$ -electrons due to the update of ion from site  $i$  to  $j$ . The probability that the ion stays put is  $p_{i \rightarrow i} = 1 - \sum_j p_{i \rightarrow j}$ .

The electron free-energy can be computed using either ED or more efficient techniques such as kernel polynomial method [41–44]. However, the quantum kMC simulation described above is very time-consuming for large systems,

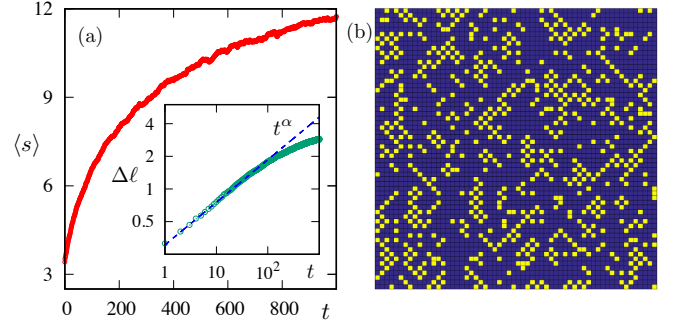


FIG. 2. (Color online) (a) Average size  $\langle s \rangle$  of checkerboard cluster as a function of time obtained from ML-kMC on a  $150 \times 150$  lattice. The inset shows the time dependence of the characteristic length scale  $\ell(t) = \ell_0 + \Delta\ell$ , where  $\ell = \langle s \rangle^{1/2}$ . The dashed line indicates a power-law growth with exponent  $\alpha \approx 0.35$ . Here time is measured in terms of 100 MC steps. (b) A close-up view of ion configuration at  $t = 800$  after quench.

since one needs to solve the electron tight-binding problem four times at every time-step in order to update just one ion. To overcome this computational bottleneck, we apply the machine learning (ML) methods that have been exploited to improve efficiency of quantum molecular dynamics simulations [45–50]. Similar approaches have also been used to enable large-scale quantum spin dynamics in double-exchange systems [51, 52]. The central idea of our approach, summarized in Fig. 1(a), is based on the principle of locality [53, 54], which, in our case, indicates that the energy change  $\Delta E_{i \rightarrow j}$  depends only on ion configuration in the neighborhood of the local update.

To implement this idea, we first translate the local ion configuration  $\{w_j\}$  into effective coordinates  $\{G_\ell\}$  that are invariant under symmetry operations of the  $D_4$  lattice point group [55]. These generalized coordinates, also known as feature variables, are then fed into a neural network (NN). Due to the discrete binary nature of ionic variables, a convolutional NN is used to enhance recognition of major features in the input. The output from the convolutional layers then propagates to a fully connected feed-forward NN, which in turn produces the predicted energy differences  $\Delta E_{i \rightarrow j}$ . We have built an eight-layer NN model trained by dataset obtained from ED-kMC simulations on a  $30 \times 30$  lattice [56]. As shown in Fig. 1(b), the ML-predicted energy changes agree well with the exact values. We further show that ionic correlation function  $C_{ij} = \langle w_i w_j \rangle$  obtained from kMC simulations based on the NN-model also agrees well with that of exact kMC simulations; see Fig. 1(c).

With the properly benchmarked NN energy model, we perform large-scale ML-kMC simulations on the FK model with up to  $10^5$  lattice sites. Our goal is to study the growth dynamics of checkerboard clusters after a temperature quench. To this end, we consider slightly electron-doped system with a filling fraction  $\rho_e = 0.55$ ,

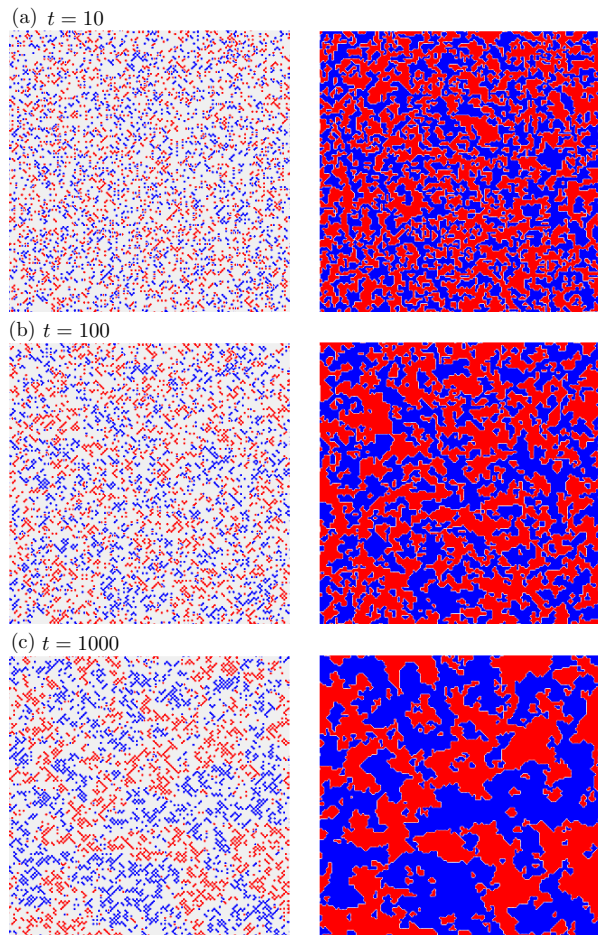


FIG. 3. (Color online) Left: snapshots of ion configuration obtained from kMC simulations of phase separation in a  $150 \times 150$  square-lattice FK model. The blue and red dots indicate ions on the A- and B-sublattice, respectively. Right: configurations of Ising variables  $\sigma_i$  that characterize the  $Z_2$ -symmetry-breaking domains associated with super-clusters.

and a low ion density  $\rho_i = 0.187$ . The repulsive interaction is set at  $U = 2$ . The low temperature phase corresponding to these parameters is a phase-separated mixture of checkerboard ordering of ions and electrons, and ion-free region with uniform electron density [35]. Some stripe orders have also been observed. In our simulations, the system is initially prepared in a state with random ionic distribution, and the temperature is suddenly reduced to  $T = 0.05$ . A snapshot of the ion configuration shown in Fig. 2(b) clearly displays several checkerboard clusters and some diagonal stripes of ions.

As the ions aggregate to form checkerboard clusters during the relaxation, the increase of average cluster size  $\langle s \rangle$  with time is shown in Fig. 2(a). Since the number of ions is conserved, the growth of checkerboard domains is similar to the phase separation of a conserved order parameter which is expected to follow a power-law scaling with an exponent  $\alpha = 1/3$ , as predicted by the Lifshitz-Slyozov-Wagner (LSW) theory [57, 58], or the model-

B dynamical model [25, 59]. As shown in the inset of Fig. 2(a), the typical length scale of checkerboard clusters indeed increases according to a power-law  $\ell = \ell_0 + \text{const} \times t^\alpha$ , where  $\alpha \approx 0.35$ , even early in the phase-separation process. However, this power-law regime only lasts a short duration and the growth slows down significantly at late stage.

This stagnation of domain-growth cannot be attributed to finite size effect since the average cluster size is still much smaller than the system sizes at late times. Instead, the freezing of checkerboard clusters is caused by a sublattice symmetry breaking hidden in the phase separation process. To illustrate this effect, we use different colors to label ions at the two sublattices of the square lattice. As shown in left column of Fig. 3, while the sizes of checkerboard clusters remain small, ions residing on the same sublattice tend to stick together, thus forming super-cluster of checkerboards. The emergence of the super-clusters is related to the broken symmetry between the A- and B-sublattices, and can be described by a  $Z_2$  order-parameter.

To further illustrate the broken  $Z_2$  symmetry associated with the super-clusters, we introduce an Ising variable  $\sigma_i$  at every lattice site such that  $\sigma_i = +1$  ( $-1$ ) if the ion closest to site- $i$  belongs to sublattice-A (B). As shown in the right column of Fig. 3, the clustering of checkerboards into super-clusters thus corresponds to the growth of Ising ferromagnetic domains. The order parameter describing this  $Z_2$  symmetry-breaking is then given by the magnetization density of Ising spins, i.e.  $\phi = \langle \sigma_i \rangle$ . It is worth noting that the order-parameter  $\phi$  is not conserved in the kMC dynamics of ions. Phenomenologically, such non-conserved field is governed by the time-dependent Ginzburg-Landau equation (TDGL) or model-A dynamics [25]. The resultant domain-coarsening is characterized by the  $L \sim t^{1/2}$  Allen-Cahn power law [18, 19]. However, as we will show next, the coarsening of Ising domains does not follow the expected power-law due to an unusual self-confinement of the ions.

To characterize the domain-growth of super-clusters, we first compute the structure factor of the Ising spins:  $S(\mathbf{k}, t) = \left| \frac{1}{N} \sum_i \sigma_i(t) \exp(i\mathbf{k} \cdot \mathbf{r}_i) \right|^2$ . The ferromagnetic ordering implies that  $S(\mathbf{k}, t)$  exhibits a growing peak at  $\mathbf{k} = 0$ . The inverse of the width of this peak can be used as a measure of the characteristic length scale of the super-clusters:  $L^{-1}(t) \sim \frac{2\pi}{\Delta k} = \sum_{\mathbf{k}} S(\mathbf{k}, t) |\mathbf{k}| / \sum_{\mathbf{k}} S(\mathbf{k}, t)$ . Interestingly, as evidenced by the nice data-point collapsing in Fig. 4(a), the coarsening of the Ising domains exhibits dynamical scaling, i.e.  $S(\mathbf{k}, t) = L^2(t) \mathcal{G}[|\mathbf{k}|L(t)]$ , where  $\mathcal{G}(x)$  is a universal scaling function. The  $1/k^3$  power-law tail at large momentum, consistent with the 2D Porod's law [20], results from the sharp interfaces between the two Ising domains.

The characteristic length  $L(t)$  extracted from the structure factor is shown in Fig. 4(b) as a function of time for three different lattice sizes. Interestingly, ex-



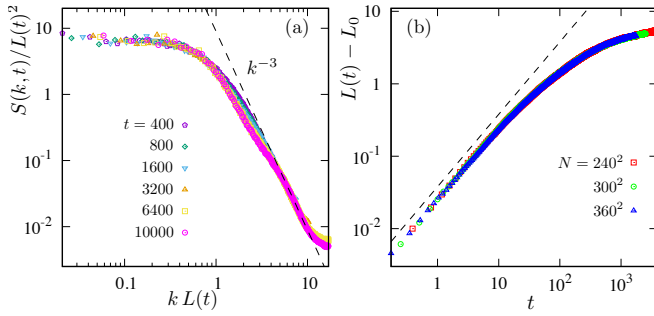


FIG. 4. (Color online) (a) Scaling plot of the time-dependent structure factor  $S(\mathbf{k}, t)$  obtained from Fourier transform of the  $Z_2$  order parameter. The dashed line shows the  $k^{-3}$  Porod's law in 2D. (b) Characteristic length  $L(t)$  of the super-clusters as a function of time for three different lattice sizes. The dashed line indicates the linear growth  $\Delta L(t) \sim t$ .

cept for a short initial period (up to  $t \sim 10$ ), the growth of this length scale does not follow the expected power law, especially at late times. Moreover, even the initial seemingly power-law growth is not consistent with the  $\alpha = 1/2$  Allen-Cahn law. Instead,  $L$  seems to increase linearly with time initially. To understand this anomalous behavior, we note that the TDGL equation or the Allen-Cahn theory describe an interface-controlled domain growth where the interfacial velocity is proportional to the curvature [60]. On the other hand, since the  $Z_2$  order parameter in our case is defined by whether the aggregating ions are on A- or B-sublattice, the domain growth exhibits an avalanche-like behavior in which ions belonging to the same checkerboard cluster shift from one sublattice to another via a nearest-neighbor hopping. A faster linear growth of the super-clusters thus arises from such avalanche dynamics at the early stage. As will be discussed below, such collective behavior can be induced by the effective non-local ion-ion interaction.

Although the ion-electron repulsion is local, the ions experience an effective long-range interaction mediated by the itinerant  $c$ -electrons. In particular, due to this non-local interaction, the emergence of a checkerboard cluster creates a staggered potential in its neighborhood that takes alternating values on neighboring sites of the bipartite lattice. This effective potential is illustrated in Fig. 5 where a test ion is placed in the neighborhood of a checkerboard cluster at the center. Exact MC simulation was used to obtain the frequency  $f_i$  that the test ion stays at site  $i$ , from which the potential is computed:  $V_i = -k_B T \log f_i$ . Importantly, this short-ranged staggered potential renders the neighborhood attractive for checkerboard of the same polarity, thus leading to the formation and growth of super-clusters.

At late stage of the phase separation, a much slower logarithmic-like growth sets in for super-clusters, as shown in Fig. 4(b). Interestingly, exactly the same staggered potential is also responsible for the stalled growth

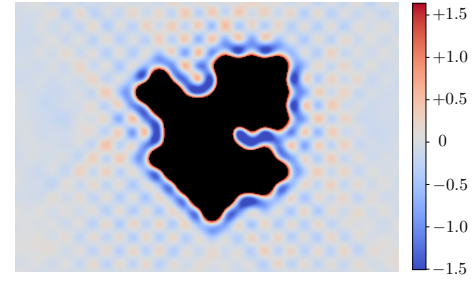


FIG. 5. (Color online) Density plot of effective potential  $V(\mathbf{r}_i) = -k_B T \log f_i$  for ions created by a checkerboard cluster at the center.

of the Ising domains and, in fact, of the smaller checkerboard clusters too. As more and more checkerboards merge to form a larger super-cluster, the staggered potential of the associated Ising domain becomes so strong that individual ions are deeply trapped at one sublattice and cannot hop to the neighboring sites. For example, consider a test ion sitting at a site that belong to the lower-energy A-sublattice in Fig. 5. Although the checkerboard at the center has a strong affinity to the new particle, as evidenced by the rather low potential energy at the edge of the cluster, the large energy barrier at B-sublattice prevents the ion from joining the cluster. The reduced mobility of ions thus results in an arrested phase separation.

To summarize, by performing the first-ever large-scale kinetic Monte Carlo simulation on the well-studied FK model, we discover a novel phase-ordering phenomenon where domain coarsening occurs simultaneously at two different scales: the growth of checkerboard clusters and the widening of Ising domains associated with a hidden broken sublattice symmetry. The competition of these two processes leads to an anomalously slow phase separation. Several interesting dynamical phenomena, such as the early-stage avalanche domain growth and the decelerated coarsening of super clusters, require further investigation and will be left for future work.

Unusual domain-coarsening has been reported in classical systems, which is often related to frustrated interactions or quenched disorder [61–65]. In this work we describe a new freezing mechanism which arises from the interaction of itinerant  $c$ -electrons and classical  $f$ -electrons or “ions”. Similar glassy dynamics could be generic for phase ordering in other correlated electron systems. A characteristic feature of correlated electron materials is the coexistence of fast electron quasiparticles and slow bosonic or collective degrees of freedom. The nontrivial interplay between these two sets of variables could lead to novel dynamical phenomena that are unique to correlated electrons. Given the complexity of such systems, we envision ML techniques as indispensable tool for multi-scale modeling of nonequilibrium dynamics driven by electron correlation effect.

*Acknowledgements.* The work was supported by the US Department of Energy Basic Energy Sciences under Contract No. DE-SC0020330. The authors also acknowledge the support of Advanced Research Computing Services at the University of Virginia.

- 
- [1] E. Dagotto, *Nanoscale phase separation and colossal magnetoresistance* (Berlin, Springer 2002).
  - [2] E. Dagotto, Complexity in strongly correlated electronic systems, *Science* **309**, 257 (2005).
  - [3] A. Moreo, S. Yunoki, and E. Dagotto, Phase separation scenario for manganese oxides and related materials, *Science* **283**, 2034 (1999).
  - [4] E. Dagotto, T. Hotta, A. Moreo, Colossal magnetoresistant materials: The key role of phase separation, *Phys. Rep.* **344**, 1 (2001).
  - [5] N. Mathur and P. Littlewood, Mesoscopic texture in manganites, *Phys. Today* **1**, 25 (2003).
  - [6] S. A. Kivelson, E. Fradkin, and V. J. Emery, Electronic liquid-crystal phases of a doped Mott insulator, *Nature* **393**, 550 (1998).
  - [7] S. A. Kivelson, I. P. Bindloss, E. Fradkin, V. Oganessian, J. M. Tranquada, A. Kapitulnik, and C. Howald, How to detect fluctuating stripes in the high-temperature superconductors, *Rev. Mod. Phys.* **75**, 1201 (2003).
  - [8] E. Fradkin, S. A. Kivelson, and J. M. Tranquada, Theory of intertwined orders in high temperature superconductors, *Rev. Mod. Phys.* **87**, 457 (2015).
  - [9] P. B. Visscher, Phase separation instability in the Hubbard model, *Phys. Rev. B* **10**, 943 (1974).
  - [10] H. J. Schulz, Domain walls in a doped antiferromagnet, *J. Phys. France* **50**, 2833 (1989).
  - [11] J. Zaanen and O. Gunnarsson, Charged magnetic domain lines and the magnetism of high- $T_c$  oxides, *Phys. Rev. B* **40**, 7391 (1989).
  - [12] V. J. Emery, S. A. Kivelson, and H. Q. Lin, Phase separation in the t-J model, *Phys. Rev. Lett.* **64**, 475 (1990).
  - [13] L. Gehlhoff, Phase separation in the one-band Hubbard model, *J. Phys. Condens. Matter* **8**, 2851 (1996).
  - [14] S. White and D. Scalapino, Phase separation and stripe formation in the two-dimensional t-J model: A comparison of numerical results, *Phys. Rev. B* **61**, 6320 (2000).
  - [15] C.-H. Yee and L. Balents, Phase separation in doped Mott insulators, *Phys. Rev. X* **5**, 021007 (2015).
  - [16] J. D. Gunton, M. San Miguel, and P. S. Saint, *The dynamics of first order phase transitions*, in “Phase Transitions and Critical Phenomena”, edited by C. Domb and J. L. Lebowitz, vol. 8, pp.269-466 (Academic, New York, 1983).
  - [17] P. L. Krapivsky, S. Redner and E. Ben-Naim, *A Kinetic View of Statistical Physics* (Cambridge University Press, 2010).
  - [18] A. J. Bray, Theory of phase-ordering kinetics, *Adv. Phys.* **43**, 357 (1994).
  - [19] A. Onuki, *Phase Transition Dynamics* (Cambridge University Press, Cambridge, UK, 2002).
  - [20] S. Puri and V. Wadhawan, Ed. *Kinetics of Phase Transitions* (CRC Press, Taylor & Francis Group, London, 2009).
  - [21] Y. Oono and S. Puri, Study of phase-separation dynamics by use of cell dynamical systems. I. Modeling, *Phys. Rev. A* **38**, 434 (1988).
  - [22] J. D. Gunton, R. Toral, and A. Chakrabarti, Numerical studies of phase separation in models of binary alloys and polymer blends, *Phys. Scr.* **T33**, 12 (1990).
  - [23] R. Weinkamer, P. Fratzl, H. S. Gupta, O. Penrose, and J. L. Lebowitz, Using kinetic Monte Carlo simulations to study phase separation in alloys, *Phase. Trans.* **77**, 433 (2004).
  - [24] L.-Q. Chen, Phase-field models for microstructure evolution, *Annu. Rev. Mater. Res.* **32**, 113 (2002).
  - [25] P. C. Hohenberg and B. I. Halperin, Theory of dynamic critical phenomena, *Rev. Mod. Phys.* **49**, 435 (1977).
  - [26] H. Furukawa, A dynamic scaling assumption for phase separation, *Adv. Phys.* **34**, 703 (1985).
  - [27] L. M. Falicov and J. C. Kimball, Simple model for semiconductor-metal transitions:  $\text{SmB}_6$  and transition-metal oxides, *Phys. Rev. Lett.* **22**, 997 (1969).
  - [28] J. Hubbard, Electron correlations in narrow energy bands, *Proc. R. Soc. A* **276**, 238 (1963).
  - [29] J. K. Freericks and V. Zlatić, Exact dynamical mean-field theory of the Falicov-Kimball model, *Rev. Mod. Phys.* **75**, 1333 (2003).
  - [30] T. Kennedy and E. H. Lieb, An itinerant electron model with crystalline or magnetic long range order, *Physica A* **138**, 320 (1986).
  - [31] J. K. Freericks, E. H. Lieb, and D. Ueltschi, Phase Separation due to Quantum Mechanical Correlations, *Phys. Rev. Lett.* **88**, 106401 (2002).
  - [32] J. K. Freericks and R. Lemański, Segregation and charge-density-wave order in the spinless Falicov-Kimball model, *Phys. Rev. B* **61**, 13438 (2000).
  - [33] G. I. Watson and R. Lemanski, The ground-state phase diagram of the two-dimensional Falicov-Kimball model, *J. Phys.: Condens. Matter* **7**, 9521 (1995).
  - [34] R. Lemański, J. K. Freericks, and G. Banach, Stripe Phases in the Two-Dimensional Falicov-Kimball Model, *Phys. Rev. Lett.* **89**, 196403 (2002); Charge stripes due to electron correlations in the two-dimensional spinless Falicov-Kimball Model, *J. Stat. Phys.* **116**, 699 (2004).
  - [35] M.-T. Tran, Inhomogeneous phases in the Falicov-Kimball model: Dynamical mean-field approximation, *Phys. Rev. B* **73**, 205110 (2006).
  - [36] M. M. Maška and K. Czajka, Pattern formation in the Falicov-Kimball model, *Phys. Stat. Sol. (b)* **242**, 479 (2005).
  - [37] M. M. Maška and K. Czajka, Thermodynamics of the two-dimensional Falicov-Kimball model: A classical Monte Carlo study, *Phys. Rev. B* **74**, 035109 (2006).
  - [38] A. E. Antipov, Y. Javanmard, P. Ribeiro, and S. Kirchner, Interaction-Tuned Anderson versus Mott Localization, *Phys. Rev. Lett.* **117**, 146601 (2016).
  - [39] G. T. Barkema, Monte Carlo Simulations of Domain Growth, in *Kinetics of Phase Transitions* Ed. S. Puri and V. Wadhawan, Chap. 3, p.101 (CRC Press, Taylor & Francis Group, London, 2009).
  - [40] D. Marx and J. Hutter, *Ab initio molecular dynamics: basic theory and advanced methods* (Cambridge University Press, Cambridge, 2009).
  - [41] N. Furukawa and Y. Motome, Order  $N$  Monte Carlo Algorithm for Fermion Systems Coupled with Fluctuating Adiabatical Fields, *J. Phys. Soc. Jpn.* **73**, 1482 (2004).
  - [42] G. Alvarez, C. Sen, N. Furukawa, Y. Motome, and E. Dagotto, The truncated polynomial expansion Monte

- Carlo method for fermion systems coupled to classical fields: a model independent implementation, *Comput. Phys. Commun.* **168**, 32 (2005).
- [43] A. Weisse, G. Wellein, A. Alvermann, and H. Fehske, The kernel polynomial method, *Rev. Mod. Phys.* **78**, 275 (2006).
  - [44] Z. Wang, G.-W. Chern, C. D. Batista, and K. Barros, Gradient-based stochastic estimation of the density matrix, *J. Chem. Phys.* **148**, 094107 (2018).
  - [45] J. Behler and M. Parrinello, Generalized Neural-Network Representation of High-Dimensional Potential-Energy Surfaces, *Phys. Rev. Lett.* **98**, 146401 (2007).
  - [46] A. P. Bartók, M. C. Payne, R. Kondor, G. Csányi, Gaussian Approximation Potentials: The Accuracy of Quantum Mechanics, without the Electrons, *Phys. Rev. Lett.* **104**, 136403 (2010).
  - [47] Z. Li, J. R. Kermode, and A. De Vita, Molecular Dynamics with On-the-Fly Machine Learning of Quantum-Mechanical Forces, *Phys. Rev. Lett.* **114**, 096405 (2015).
  - [48] J. S. Smith, O. Isayev, and A. E. Roitberg, ANI-1: an extensible neural network potential with DFT accuracy at force field computational cost, *Chem. Sci.* **8**, 3192 (2017).
  - [49] L. Zhang, J. Han, H. Wang, R. Car, and Weinan E, Deep Potential Molecular Dynamics: A Scalable Model with the Accuracy of Quantum Mechanics, *Phys. Rev. Lett.* **120**, 143001 (2018).
  - [50] H. Suwa, J. S. Smith, N. Lubbers, C.D. Batista, G.-W. Chern, and K. Barros, Machine learning for molecular dynamics with strongly correlated electrons, *Phys. Rev. B* **99**, 161107 (2019).
  - [51] P. Zhang, P. Saha, and G.-W. Chern, Machine learning dynamics of phase separation in correlated electron magnets, *arXiv:2006.04205* (2020).
  - [52] P. Zhang and G.-W. Chern, Arrested phase separation in double-exchange models: machine-learning enabled large-scale simulation, *arXiv:2105.08221* (2021)
  - [53] K. Walter, Density functional and density matrix method scaling linearly with the number of atoms, *Phys. Rev. Lett.* **76**(17), 3168.
  - [54] E. Prodan, and K. Walter, Nearsightedness of electronic matter, *Proc. Natl. Acad. Sci. U.S.A.* **102**.33 (2005): 11635-11638.
  - [55] J. Ma, P. Zhang, Y. Tan, A. W. Ghosh, and G.-W. Chern, Machine learning electron correlation in a disordered medium, *Phys. Rev. B* **99**, 085118 (2019).
  - [56] Details of the neural network structure, dataset selection, and training process can be found in the supplemental information.
  - [57] I. M. Lifshitz and V. V. Slyozov, The kinetics of precipitation from supersaturated solid solutions, *J. Phys. Chem. Solids* **19**, 35 (1961).
  - [58] C. Wagner, Theorie der Alterung von Niederschlagen durch Umlosen, *Z. Elektrochem* **65**, 581 (1961).
  - [59] J. W. Cahn and J. E. Hilliard, Free Energy of a Nonuniform System. I. Interfacial Free Energy, *J. Chem. Phys.* **28**, 258 (1958).
  - [60] S. M. Allen and J. W. Cahn, A microscopic theory for antiphase boundary motion and its application to antiphase domain coarsening, *Acta Metall.* **27**, 1085 (1979).
  - [61] J. D. Shore, M. Holzer, J. P. Sethna, Logarithmically slow domain growth in nonrandomly frustrated systems: Ising models with competing interactions, *Phys. Rev. B* **46**, 11376 (1992).
  - [62] M. R. Evans, Anomalous coarsening and glassy dynamics, *J. Phys.: Condens. Matter* **14**, 1397 (2002).
  - [63] H. Tanaka, Viscoelastic phase separation, *J. Phys.: Condens. Matter* **12**, R207 (2000).
  - [64] M. Zannetti, Aging in domain growth, in: S. Puri, V. Wadhawan (Eds.), *Kinetics of Phase Transitions*, CRC Press, Boca Raton, FL, USA, 2009, p. 153;
  - [65] F. Corberi, Coarsening in inhomogeneous systems, *C. R. Physique* **16**, 332 (2015).